

AD-A955 391

Chapter 7

ELECTROMAGNETIC PULSE (EMP) PHENOMENA

The nuclear electromagnetic pulse (EMP) is the time-varying electromagnetic radiation resulting from a nuclear burst. It has a very broad frequency spectrum, ranging from near dc to several hundred MHz.

The generation of EMP from a nuclear detonation was predicted even before the initial test, but the extent and potentially serious degree of EMP effects were not realized for many years. Attention slowly began to focus on EMP as a probable cause of malfunction of electronic equipment during the early 1950s. Induced currents and voltages caused unexpected equipment failures during nuclear tests, and subsequent analysis disclosed the role of EMP in such failures. Finally in 1960 the possible vulnerability of hardened weapon systems to EMP was officially recognized. Increased knowledge of the electric and magnetic fields became desirable for both weapons diagnostics and long-range detection of nuclear detonations. For all these reasons a more thorough investigation of EMP was undertaken.

Theoretical and experimental efforts were expanded to study and observe EMP phenomenology and to develop appropriate descriptive models. A limited amount of data had been gathered on the phenomenon and its threat to military systems when all aboveground testing was halted in 1962. From this time reliance has been placed on underground testing, analysis of existing atmospheric test data, and nonnuclear simulation for experimental knowledge. Extended efforts have been made to improve theoretical models and to develop associated computer codes for predictive studies. At the same time, efforts to develop simulators capable of produc-

ing threat-level pulses for system coupling and response studies have been expanded.

This chapter describes the EMP generation mechanism and the resulting environment for various burst regimes. The description is largely qualitative, since the complexity of the calculations requires that heavy reliance be placed on computer code calculations for specific problems. Some results of computer code calculations are presented, but generalization of these results is beyond the scope of this chapter. More complete treatments of the EMP phenomena may be found in the "DNA EMP (Electromagnetic Pulse) Handbook (U)" (see bibliography).

ENVIRONMENT - GENERAL DESCRIPTION

7-1 Weapon Gamma Radiation

The gamma radiation output from a nuclear burst initiates the processes that shape the development of an electromagnetic pulse. The gamma radiation components important in EMP generation are the prompt, air inelastic, and isomeric gammas (see Chapter 5). Briefly, the prompt gammas arise from the fission or fusion reactions taking place in the bomb and from the inelastic collisions of neutrons with the weapon materials. The fraction of the total weapon energy that may be contained in the prompt gammas will vary nominally from about 0.1% for high yield weapons to about 0.5% for low yield weapons, depending on weapon design and size. Special designs might increase the gamma fraction, whereas massive, inefficient designs would decrease it. This component is generated within

Change 1 7-1

This document has been approved
for public release and sale; its
distribution is unlimited.

less than a microsecond of detonation time. High energy neutrons, which result from the fusion process, emerge from the bomb debris with energies on the order of four to fourteen MeV. For a surface or air burst, these neutrons lose their energies primarily through a large number of inelastic collisions with the surrounding air molecules over a time period of many microseconds. This gives rise to a source of gammas over the same time span. Isomeric gammas are given off by nuclei of certain fission products in decaying from excited states to the ground state. They are important at times after the peaks in prompt and air inelastic contributions (see Section 1, Chapter 5).

7-2 Compton Current

When gamma radiation from any of the sources mentioned in the preceding paragraph impinges upon air molecules, high energy electrons are created by the Compton effect. In this effect, illustrated in Figure 7-1, the incident gamma ray interacts with an electron in the shell of an atom, imparting to it a large amount of energy. Both the electron and a less energetic

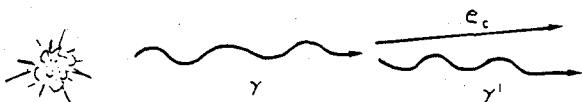


Figure 7-1. (U) The Compton Effect (U)

gamma ray scatter, primarily in the forward direction, and the scattered gamma rays frequently retain sufficient energy to repeat the process. In addition to the generation of Compton electrons, over ten percent of the gamma rays with energy above 5 MeV may generate electron-positron pairs (pair production). The

7-2 Change 1

positrons will cause ionization by inelastic collisions and eventually will be annihilated on collision with an electron, resulting in two 0.511 MeV gamma rays. The radial beams of scattered high energy electrons comprise a current termed the Compton current. If certain spatial and time conditions are met by a current, an electromagnetic field is generated. Since the prompt gamma ray pulse increases rapidly to a peak value and then decays (Section 1, Chapter 5), and since the Compton electrons lose energy as described in the following paragraph, the Compton current rises to a peak value rapidly and then decays as illustrated in Figure 7-2.

7-3 Ai. Conductivity

The high energy electrons in the Compton current lose some energy to the surrounding air molecules through inelastic collisions. The energy lost in these collisions goes into the freeing of additional electrons from the air molecules, i.e., further ionization. A drastic change in the conductivity of air takes place as it is ionized to become a plasma consisting of molecules, atoms, ions, electrons and accompanying electromagnetic radiation (see paragraph 4-2, Chapter 4). The conductivity will vary in space and time with the density and mobility of the ions and electrons, and the mobility depends on the electric field strength. Under certain conditions of air density and distance the x-rays from the bomb may contribute significantly to the air conductivity. Further complications are introduced by the recombination of ions and electrons. Initially the dominant process is the attachment of electrons to neutral oxygen molecules, reducing their mobility. Later the negative ions and electrons recombine with positive ions, reducing the charge density. Both processes, which are strongly dependent on air density, water content of the air, and the electric field, tend to reduce the conductivity of this partially ionized plasma. Figure 7-3 shows an example of air conductivity. The sudden rise at 8 microseconds



UNANNOUNCED

[Redacted]

DNA
(6-11)

Deleted

[Redacted]

Figure 7-2 Compton Current at 500 Meters from a 4200 TJ (1 Mt) Ground Burst

[Redacted]

[Redacted]

[REDACTED]

DNA
(S)(1)

Deleted

[REDACTED] Conductivity at 500 Meters from a 4200 TJ (1 Mt) Low-Altitude Burst [REDACTED]

is due to the local arrival of the neutron flux that produces ionization by nuclear reactions other than inelastic collision, namely (n,p) and (n, γ) reactions; however, earlier times are of greatest interest for the generation of EMP.

7-4 Radical Electric Field

If a nuclear burst occurs in homogeneous (constant density) atmosphere, with no geomagnetic fields present, a charge-separation model may be used to describe the resulting electric fields. Positive and negative charges are separated as the Compton electrons sweep off in a radial direction from the explosion, while the heavier ions tend to remain behind. Thus, two shells of charge are created, an inner positive ion shell and an outer shell of electrons. This separation produces a large local electric field in the radial direction shown as E_r in Figure 7-4. The magnitude of the field is limited as the air conductivity rises to permit return currents. Conductivity is higher closer to the burst where the current are more dense, so this region is the first to saturate and to limit the radial field although the radial electric field is higher when saturation occurs. These effects are depicted schematically in Figure 7-5.

It is to be noted, however, that the total current distribution and the resulting radial electric field are perfectly spherically symmetric in this hypothetical illustration. It is a fundamental property of such a current distribution that no magnetic field is generated and no electromagnetic field is radiated away. The various asymmetries that occur in practice, and the resulting fields that are generated in the source region or radiated away are discussed in the following paragraphs.

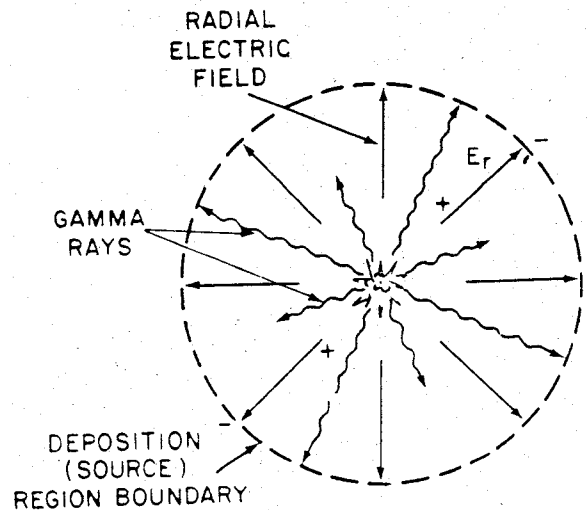


Figure 7-4. Charge Separation Model

ELECTROMAGNETIC FIELD GENERATION

7-5 Medium Altitude Air Burst

This category of nuclear explosions is defined to include weapon bursts under about 30 kilometers (19 miles) altitude, but sufficiently high that the deposition region containing the source currents does not touch the earth. In this case there are three principal factors tending to destroy the spherical symmetry of the current distribution discussed in the preceding paragraph: the atmospheric density gradient, the earth's magnetic field, and the configuration of the weapon itself. Since the earth's magnetic field is a much more important influence in less dense atmosphere, it will be discussed in succeeding paragraphs in connection with high-altitude bursts.

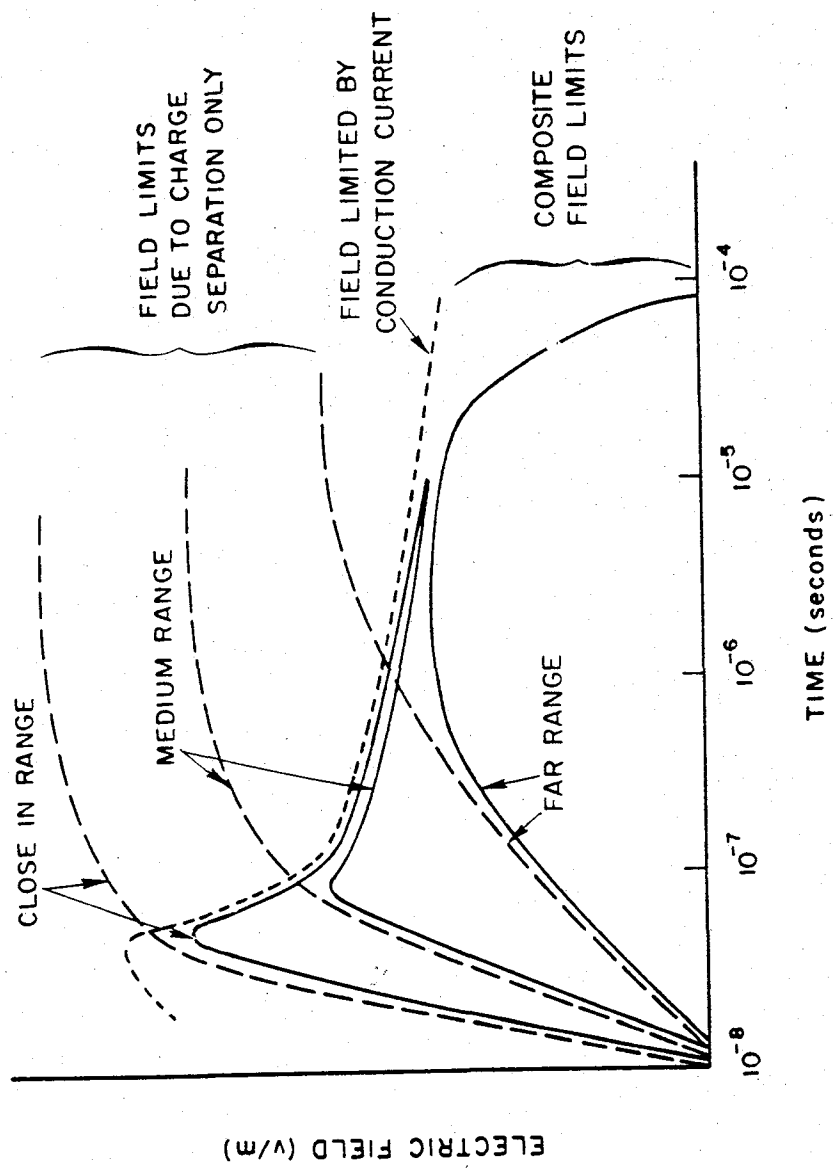


Figure 7-5. Limits on Electric Field Waveforms

[REDACTED]

The density gradient in the lower atmosphere leaves the current distribution in the deposition region symmetric in azimuth only, since the strength of all the deposition region interactions depends on the density of its constituents. Thus there is a net vertical current component, the strength of which is expressed in terms of a dipole moment. This quantity is responsible for the generation of a magnetic field in the deposition region and the radiation of an electromagnetic wave from this region. These effects are shown in Figure 7-6, assuming no weapon asymmetry. The radiation, which is in the form of a simple vertical electric dipole, is a high intensity brief pulse that includes a broad spectrum of frequencies up to many MHz. Figure 7-7 demonstrates the relationship of energy per unit frequency as a function of frequency. The electric field as a function of range, R , and azimuth, θ , follows the form

$$E(t) = \frac{R}{R_0} E_0(t) \sin \theta$$

where R_0 is the radius of the deposition region and E_0 is the time dependent electric field at R_0 . The angular dependence of radiated electromagnetic radiation is such that maximum intensity is radiated horizontally from the burst and is minimum directly above or below the burst. Simplified general waveforms of the quantities discussed here are presented in Figure 7-8.

7-6 Surface Burst

[REDACTED] DNX (6X)

The presence of the ground introduces a strong asymmetry in addition to the ones described above. The ground is a very good absorber of neutrons and gamma rays and a good conductor of electricity compared with air. Therefore, the deposition region consists approximately of a hemisphere, resulting in a very large dipole moment and consequently large radiated fields. Further, the conducting ground allows an effective return path for the electron shell near the surface with the result that current loops are formed. That is, electrons travel outward from the burst in the air, then return through the higher conductivity ground toward the burst point. These current loops form a toroidal shaped solenoid resulting in very large azimuthal magnetic fields in the deposition region, especially close to the ground. These effects are shown in Figure 7-9. Figure 7-10 shows a typical toroidal magnetic field waveform in the deposition region near the surface.

[REDACTED] There can be extremely large electric and magnetic fields as well as the presence of a highly conducting plasma within the deposition region. As a result of the number of variables that can affect the magnitude and shape of the fields, it is not possible to provide a simple description of the fields.

[REDACTED] The peak radiated electric fields are ten to a hundred times stronger than for a similar air burst. The range, R_0 , at which the radiation region begins is a function of weapon yield as shown in Table 7-1.

[REDACTED] The magnitude of the peak value of the radiated electric waveform for a surface burst is a weak function of yield, varying from about 1,300 volts per meter at R_0 for a 4.2 TJ (1KT)

DNA
(6)(1)

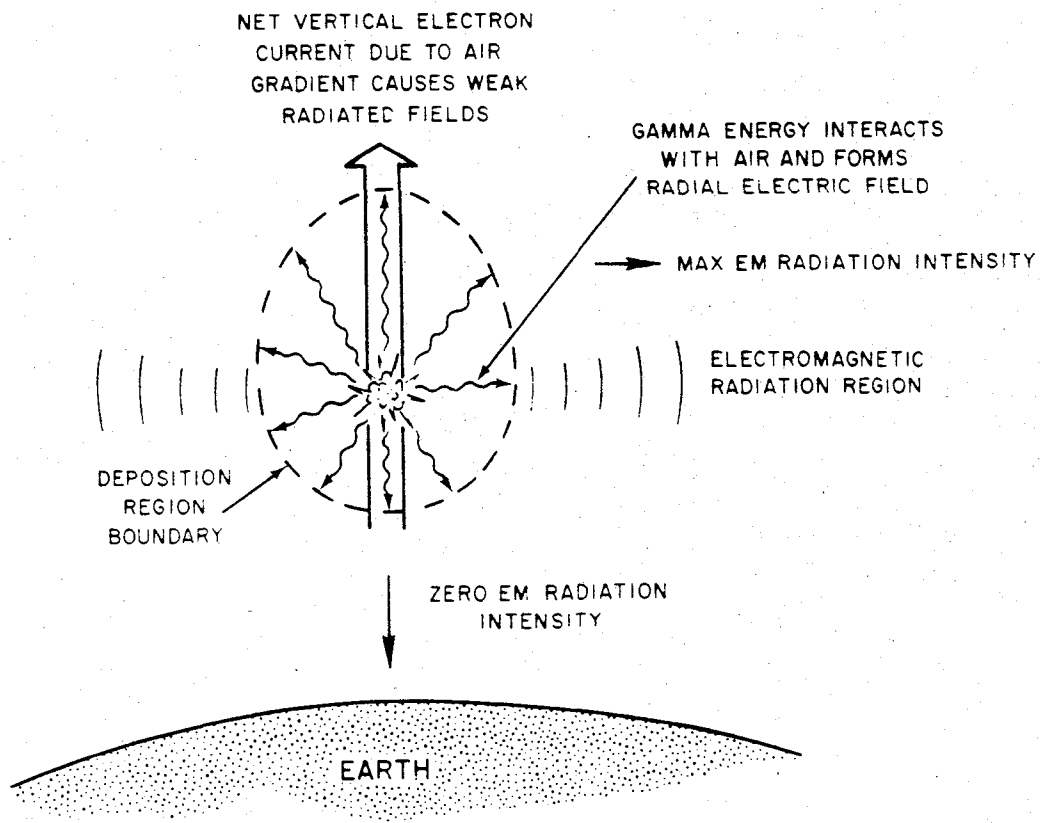


Figure 7-6. Simple Illustration of Air-Burst EMP

[REDACTED]

Deleted

DNA
(S)(1)

Figure 7-7 [REDACTED] Normalized Frequency Spectrum of the Electric-Dipole Radiated EMP for Air Bursts [REDACTED]

Change 1 7-9

[REDACTED]

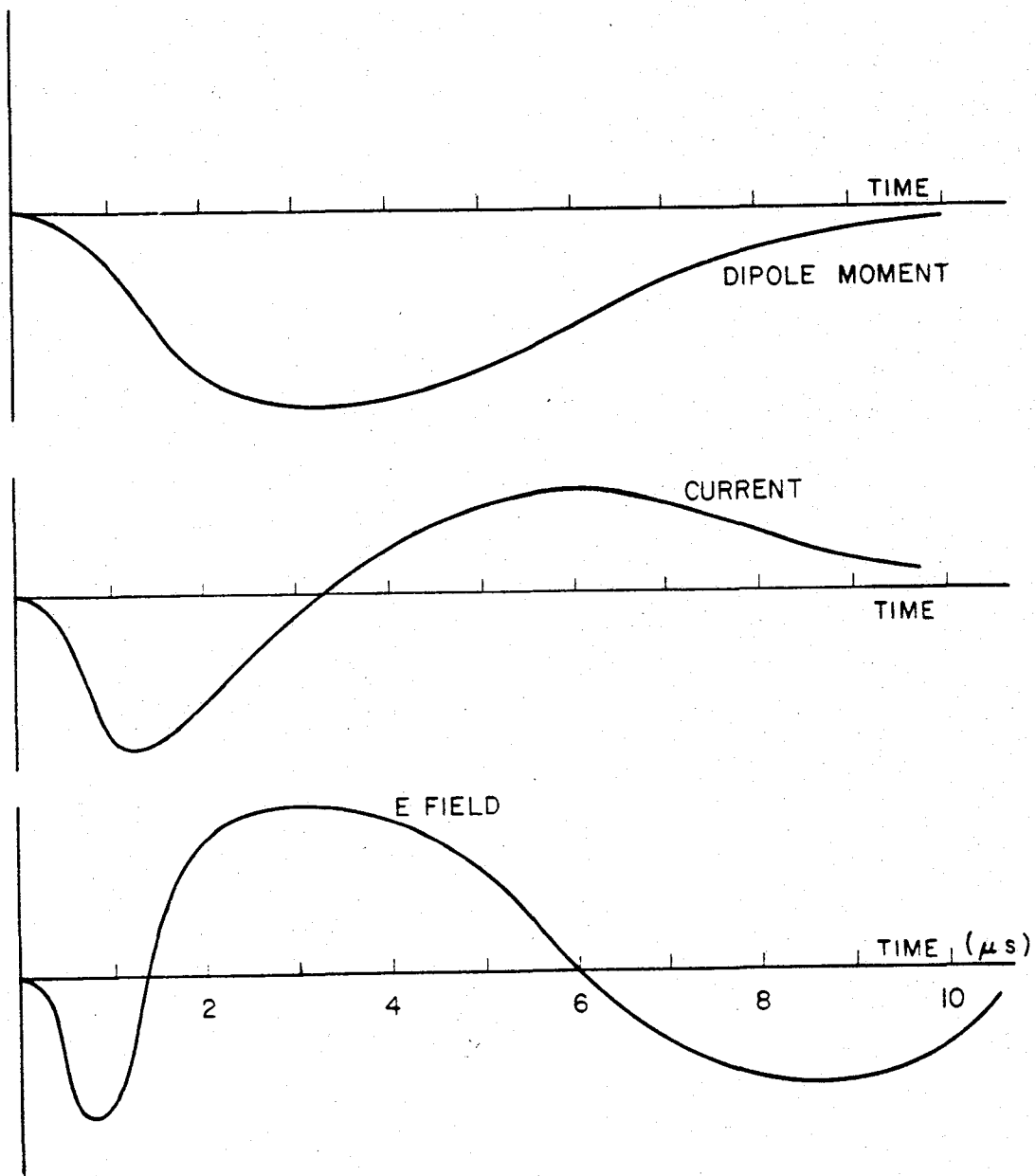


Figure 7-8 Comparison of General Waveforms for the Dipole Moment, the Current, and the E-Field for and Air Burst

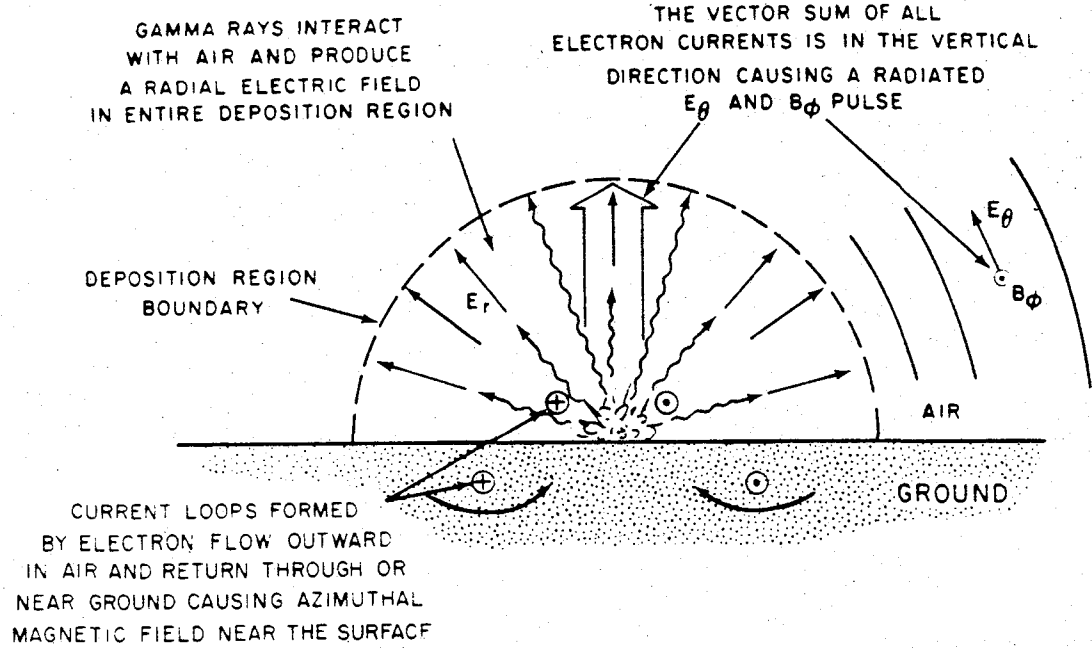


Figure 7-9 Simple Illustration of Surface Burst EMP

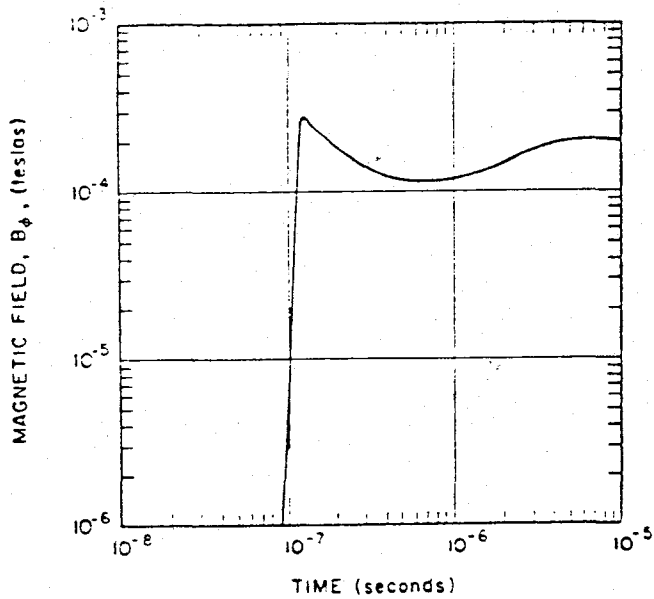


Figure 7-10 Shape of Magnetic Field for Toroid Model

explosion to about 1,670 volts per meter for a 4.2×10^4 TJ (10 MT) explosion. For most cases, a value of 1,650 volts per meter may be assumed. At ranges along the surface beyond R_0 , the peak radiated electric field varies inversely with the distance from the burst. Thus, the magnitude of the peak radiated electric field along the surface may be estimated from the equation

$$E = \frac{R_0}{R} E_0$$

where R_0 is the range to the beginning of the radiation region, R is the distance along the surface to the point of interest, E_0 is the peak value of the radiated field at R_0 (assumed to be about

Table 7-1. [REDACTED] Variation of Range, R_0 at which the Radiation Region Begins, with Yield [REDACTED]

DUR
(4)(3)

1.650 volts per meter), and E is peak value of the radiated field at R . For example, the peak electric field 10 kilometers from a 4200 TJ (1 MT) surface burst would be

$$E = \left(\frac{7.2}{10}\right) (1.650) \approx 1.200 \text{ v/m.}$$

The peak electric field at the same distance from a 420 TJ (100 KT) surface burst would be

$$E = \left(\frac{5.8}{10}\right) (1.650) \approx 950 \text{ v/m.}$$

The spatial distribution of the radiated signal involves not only the inverse range attenuation discussed above, but also the polar angle. The magnitude of the $R \cdot E_\theta$ product follows a complicated function of the polar angle, θ . Figure 7-11 shows the computed variation of the radiated EMP signals as a function of θ . The variation in the waveform shape, as well as in the peak amplitude, as a function of angle should be noted. Because of the greater rise time of the

waveforms as the vertical is approached, it is apparent that the high frequency content of the signals decreases. The frequency spectrum is an important parameter for coupling analysis. Figure 7-12 shows the normalized frequency spectrum of the horizontally radiated EMP from a surface burst. Comparing this spectrum with that shown in Figure 7-7 shows significantly greater high frequency content for the surface burst.

The preceding discussion was intended to illustrate the general characteristics of the EMP fields generated by surface bursts and the variation of the peak radiated electric fields in space. In addition to the behavior of the electric and magnetic fields, the air conductivity is important for more accurate coupling analysis. A few selected examples of these quantities are presented in later sections of this chapter; however, it is beyond the scope of this manual to provide complete EMP environmental data upon which vulnerability analyses may be based.

7-7 High Altitude Burst [REDACTED]

This burst regime is defined to include any nuclear burst at an altitude above about 30 kilometers (19 miles). In this regime the atmosphere is so sparse above the burst that relatively little Compton current is generated there. The deposition region, departing far from spherical symmetry, consists principally of a pancake shaped volume extending from about 20 to 50 kilometers (12 to 30 miles) in altitude and to the horizon as viewed from the burst. Thus, very high altitude bursts may cover vast geographical areas. A further asymmetry, the earth's magnetic field, is responsible for the form of the radiation. The Compton electrons, which result from collisions of the prompt gammas and x-rays with the air molecules in the deposition regions, are deflected by the earth's field to follow helical paths significantly long



[REDACTED]

Deleted

DNA
(6)(1)

Figure 7-11 [REDACTED] Variation of the Radiated EMP for a Surface Burst with Angle θ Measured from the Vertical in Radians [REDACTED]

[REDACTED]

[REDACTED]

DNA
(6X1)

Deleted

Figure 7-12 [REDACTED] Normalized Frequency Spectrum of the Horizontally Radiated EMP for a Surface Burst [REDACTED]

7-14 Change 1

[REDACTED]

during the time between collisions in the rare-field medium. The accelerated electrons produce the characteristic synchrotron radiation with a large high-frequency content. The peak amplitude of the electric field near the surface may be quite large, a few tens of thousands of volts/meter for high bursts. Figure 7-13 illustrates the basic geometry of this burst.

DNA
(41)

DNA
(41)

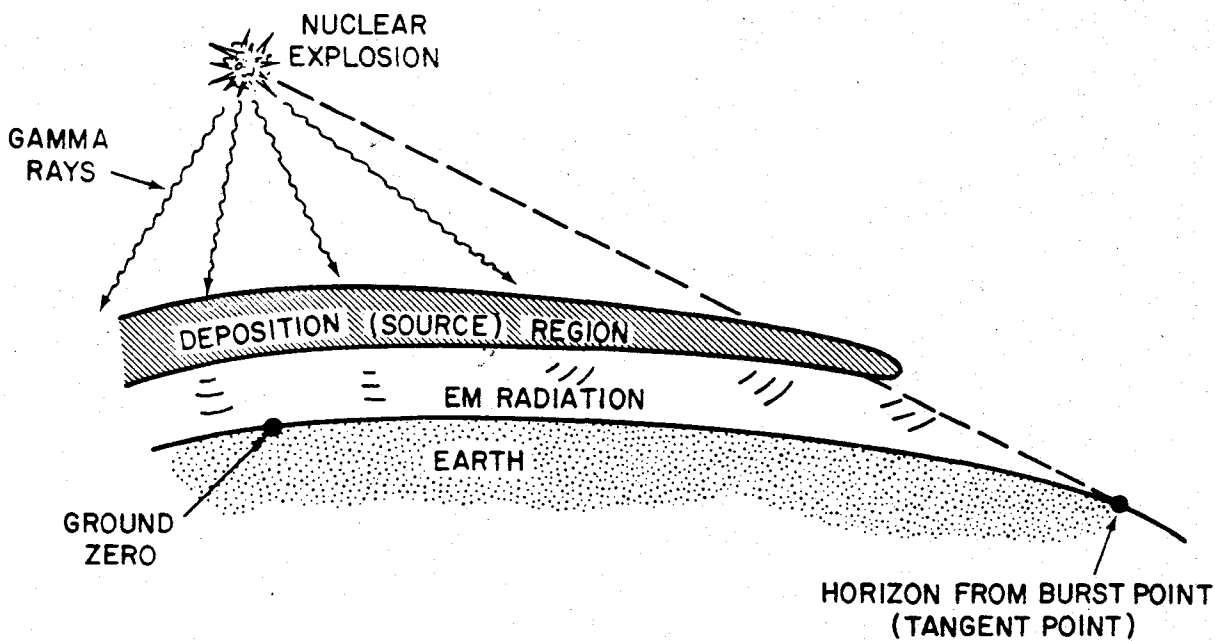


Figure 7-13 Illustration of the Basic Geometry of the High-Altitude Burst

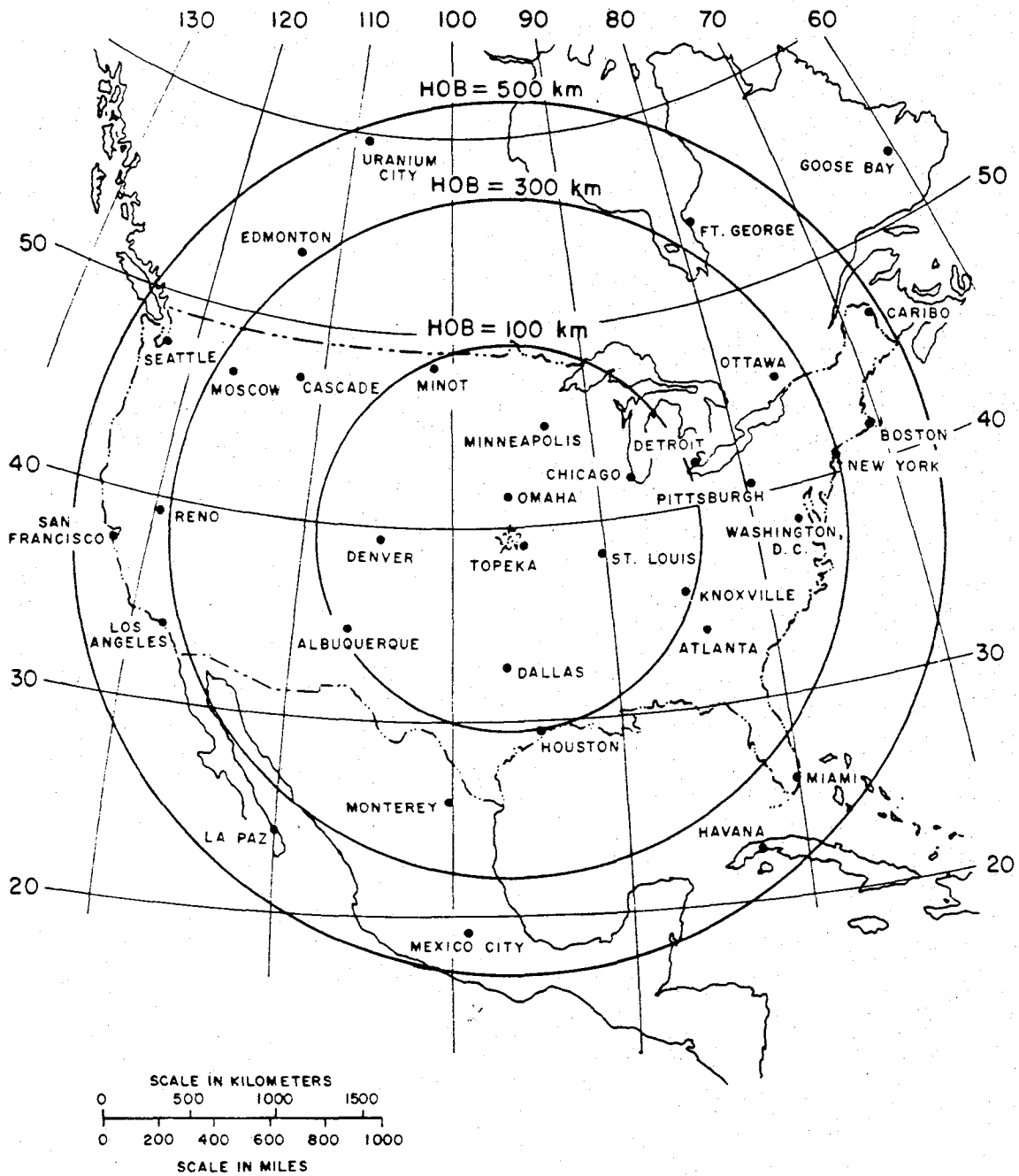


Figure 7-14 Ground Coverage for Bursts of 100, 300, and 500 km (about 62, 186, and 310 miles) for a Large Yield Burst Above the Geographical Center of the (conterminous) United States

7-16 Change 1

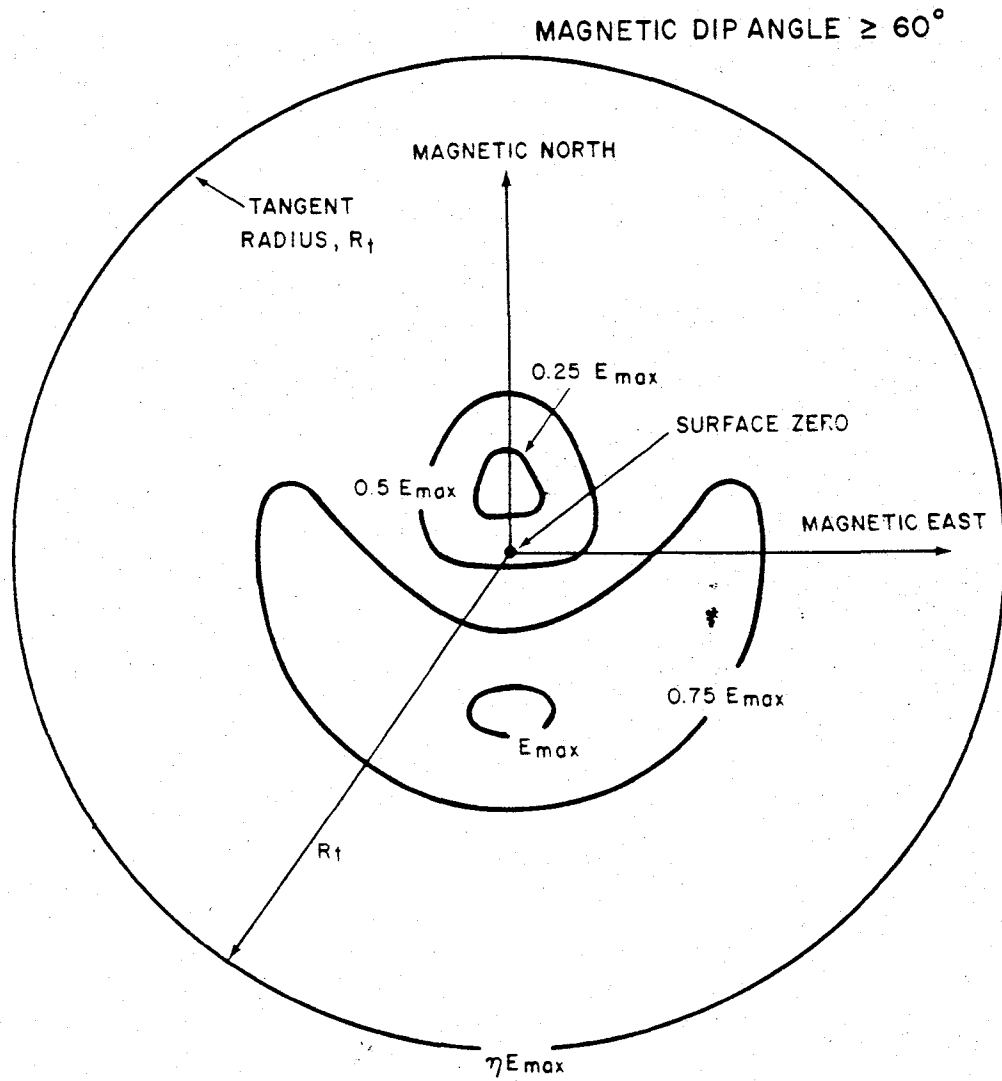
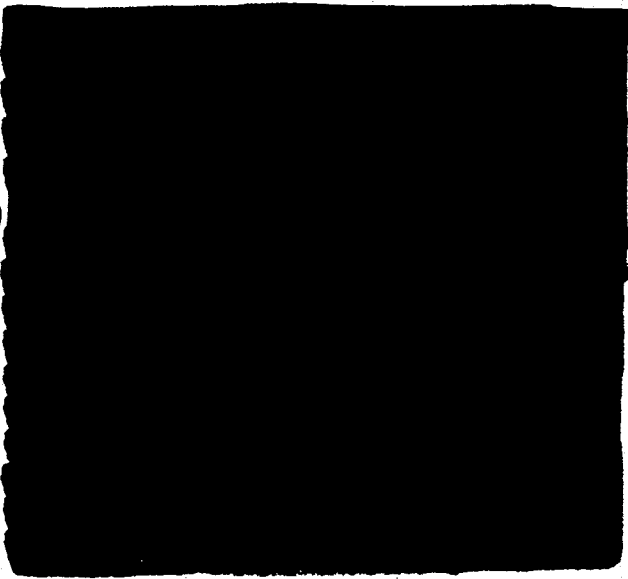


Figure 7-15 Basic Variations in Incident Peak Electric Field for Locations on the Earth's Surface for HOB above 500 km



[Redacted]

[Redacted]



DNA
(6)(3)



DNA
(6)(1)

[Redacted]

DNA
(6)(3)

Deleted

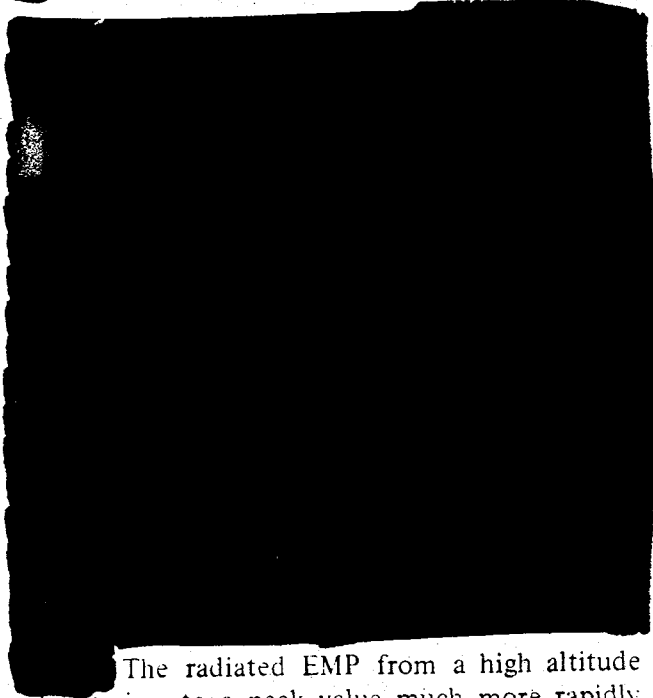
Figure 7-16 [Redacted] Maximum Peak Electric Field as a Function of Gamma Ray Yield for Selected Burst Heights [Redacted]

7-18 Change 1

[Redacted]

[Redacted]

DNA
(S)(1)



than that from a surface or low air burst. Figure 7-17 illustrates the time waveform of the radiated signal from a high altitude burst. The analytic expression

$$E(t) = 5.3 \times 10^4 (e^{-4t} - e^{-476t}) \text{ v/m}$$

where t is in microseconds, describes the waveform in Figure 7-17. The frequency spectrum of this pulse is illustrated in Figure 7-18. As the gamma yield of the weapon decreases, the pulse width tends to increase, decreasing the relative high frequency content of the signal. Similarly, increasing the angle between the line-of-sight and the vertical through the burst point increases the pulse width.

The radiated EMP from a high altitude burst rises to a peak value much more rapidly

The high altitude burst is the dominant threat to exoatmospheric systems. The most severe EMP environment for such a system comes from a line-of-sight path that passes

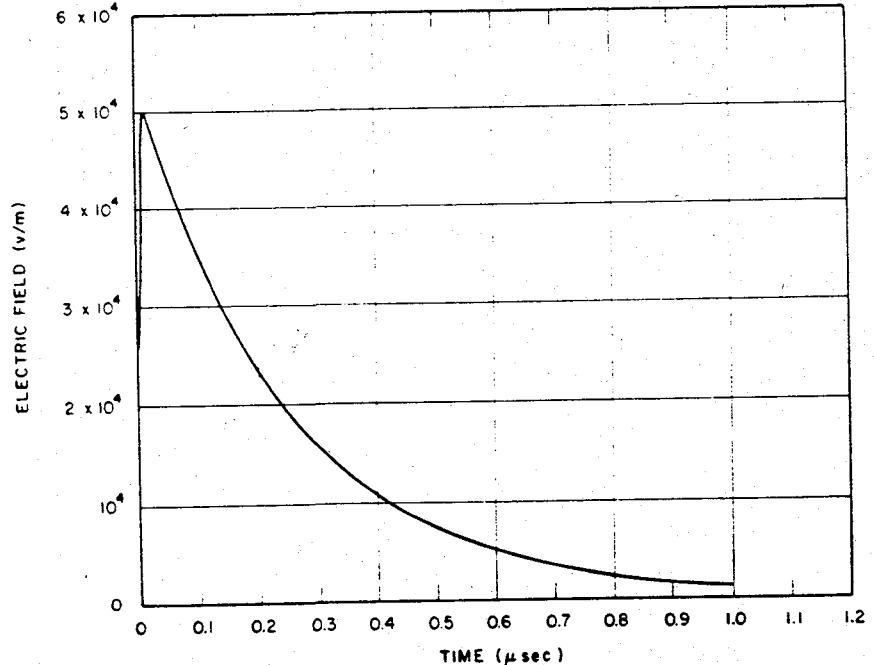


Figure 7-17 Time Waveform of High-Altitude Radiated

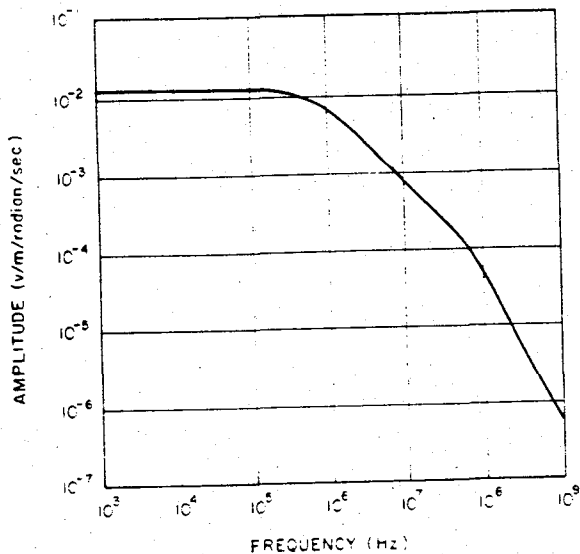


Figure 7-18 Amplitude of High-Altitude Radiated Signal

through the deposition region but misses the earth and is propagated through the ionosphere (see Figure 7-19). The ionosphere acts as a high pass filter, and only frequencies above a given cutoff are observed. The cutoff frequency depends on the altitude, time of day and sunspot activity, and, for example, varies between about 3 and 14 MHz at night, depending on the altitude of the observer. Daytime cutoff frequencies, of 30 MHz may be encountered for a 1000 km high observer. In addition, the effective index of refraction, and therefore the group velocity of the EMP signal also varies, with the higher frequencies traveling fastest. Also, the transmission for frequencies near the cutoff is very large, rising to near unity for higher frequencies. Although the amplitude of the dispersed pulse will be much smaller than that of the undispersed pulse, the signal will be stretched out greatly in

time. For frequencies above the cutoff there will be little energy loss. Figure 7-20 shows a predicted dispersed EMP (DEMP) signal from a high altitude burst as viewed by an observer at 100 km altitude. This is based on a nighttime ionosphere at sunspot minimum.

SYSTEM GENERATED EMP

7-8 General Description

The term System Generated Electromagnetic Pulse (SGEMP) refers to the fields and currents generated by the interaction of weapons-produced radiation (principally X-rays and gamma rays) with a system or portion of a system. The system generated electromagnetic pulse is produced inside or in the vicinity of a system when an incident photon pulse interacts with the material of the system. Photoelectric and Compton electrons are created, and the resulting emission current produces electric and magnetic fields. Internal EMP, or IEMP, which refers to the electromagnetic fields interior to systems and containers, and which is generally generated by gamma rays, or high energy X-rays, is included in the general category of SGEMP. SGEMP specifically excludes the internal effects associated with transient radiation effects on electronics (TREE).

The system-generated EMP is most important for electronic components in satellites and ballistic systems above the deposition region that would be exposed directly to the nuclear radiations from a high-altitude burst. The system-generated EMP can also be significant for surface and moderate-altitude bursts if the system is within the deposition region but is not subject to damage by other weapons effects. This could possibly occur for surface systems exposed to a burst of relatively low yield or for airborne (aircraft) systems and burst of higher yield.

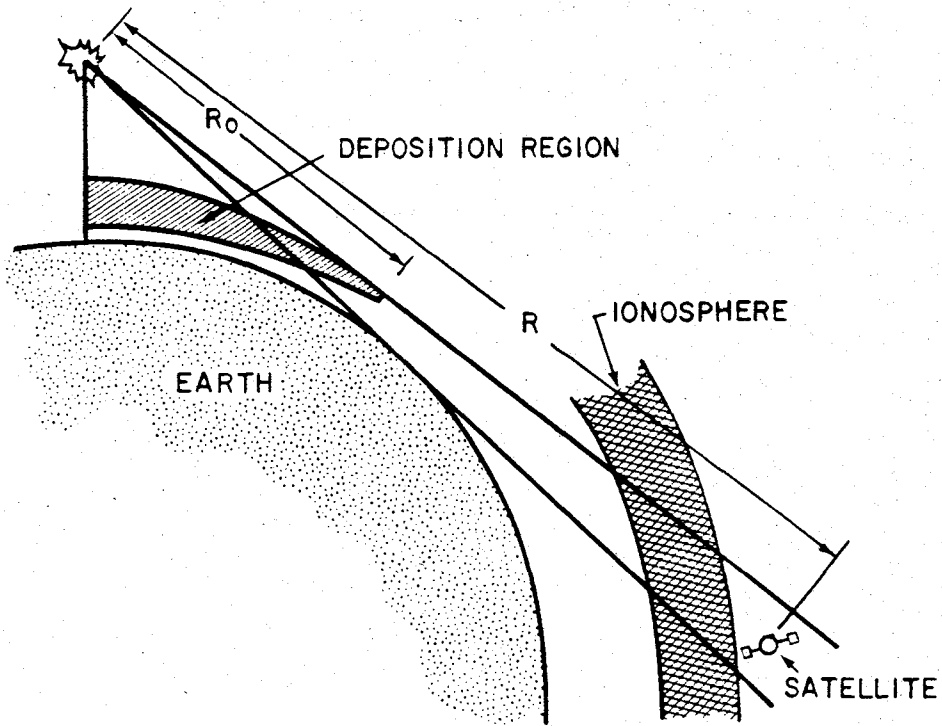


Figure 7-19 The Geometry for Producing Dispersed EMP for Exoatmospheric Systems

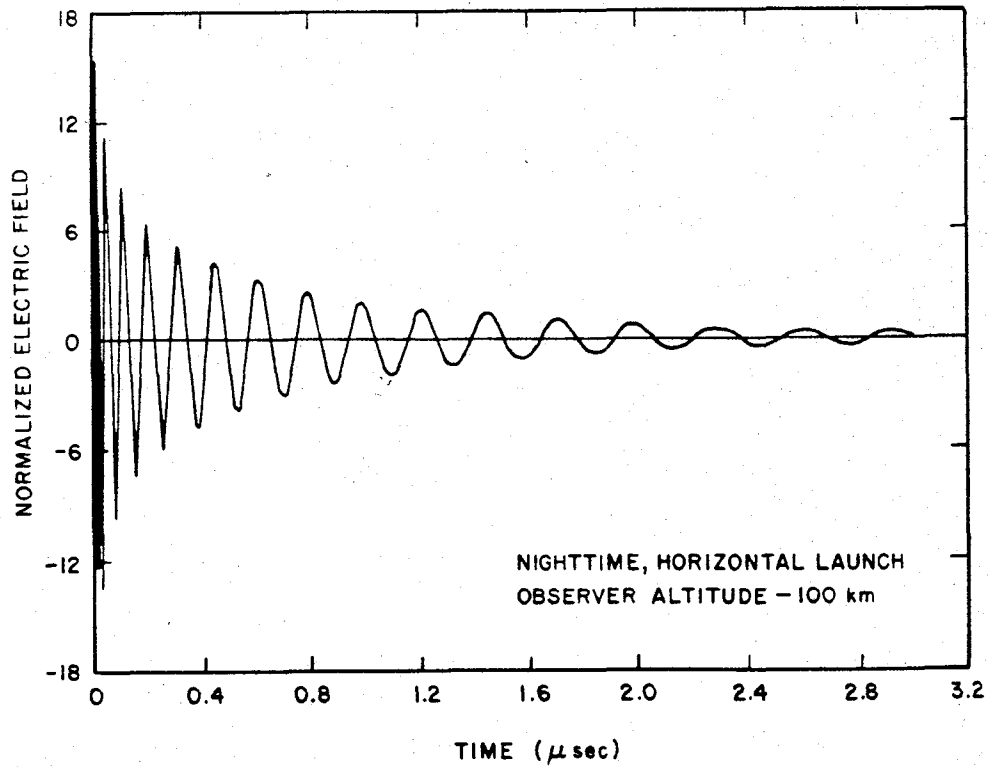


Figure 7-20 Electric Field Time Waveform of High-Altitude EMP after Dispersion by Nighttime Ionosphere

Change 1
7-21



7-9 SGEMP Generation

The generation of SGEMP is a complex function of many physical phenomena. The complexity of the problem precludes quantifying SGEMP generation for any broad class of systems. This section, therefore, will attempt to describe some of the generation phenomena for one simple problem. The "DNA EMP (Electromagnetic Pulse) Handbook," DNA 2114H-3, Volume 3, should be consulted for an in-depth treatment of the subject (see bibliography).

Figure 7-21 illustrates SGEMP generation in a cavity. The incident X-rays and gamma rays create photo- and Compton electrons, respectively, within the cavity walls. The generation is, of course, dependent on the energy flux of the incoming photons and the properties of the wall material. The photo- and Compton electrons subsequently interact with the atoms of the wall material to produce secondary electrons. Those electrons created near the surface (within an electron mean-free-path) with velocity vectors toward the surface generally will be emitted. The net electron currents, both within and without the cavity, gives rise to a magnetic field which will induce currents in circuit loops via magnetic coupling.

For this discussion, it is assumed that the electron emission and subsequent field generation are separable problems. Further, the electron emission from the external wall surfaces will be ignored. The problem under consideration is thus one in which electrons are emitted from two internal surfaces of the cavity in the forward and reverse directions, the emission being described as a time and energy dependent electron flux.

As the emitted electrons traverse the cavity, a net forward current will be observed within the cavity while a space charge is established concurrently. If the cavity is at vacuum or

near-vacuum conditions ($0.13 \text{ pascal} - 10^{-3} \text{ Torr}$ or less) and of appropriate size, space charge limitation will occur. This will result in the creation of high electric fields ($10^5 - 10^6 \text{ volts/meter}$) near the walls.

If the cavity pressure is above 0.13 pascal , another phenomenon will occur in sufficient intensity to alter the SGEMP. The emission electrons will interact with the gas molecules to produce additional secondary electrons (hereafter called gas electrons) and positive ions. The gas electrons will tend to "stream" to the cavity walls in comparison to the heavier and slower gas ions that are created concurrently. The gas ions will neutralize the space charge, thereby allowing more electrons to traverse the cavity. Thus the E-field intensity near the walls will decrease while the current in the cavity, and concurrently the magnetic field, will increase. It should be noted that quantitative analysis of the electron emission and subsequent SGEMP generation for even this simple problem requires the use of complex computer codes on large computers.

7-10 Problem Definition

It is emphasized that the above discussion dwells on only *one* small aspect of the SGEMP problem: the generation of an idealized SGEMP in a simplified geometry. A complete treatment of the SGEMP for a given system must start with the threat definition and the incoming photon flux. This must then be translated into electron emission from all surfaces, cables, components, etc., of the system. From the emission, fields and currents throughout and external to the system must be determined in a self-consistent manner. Next, coupling of the fields and currents to the system electronics must be established. Finally, the reaction of the electronics to the coupled energy must be determined and evaluated.

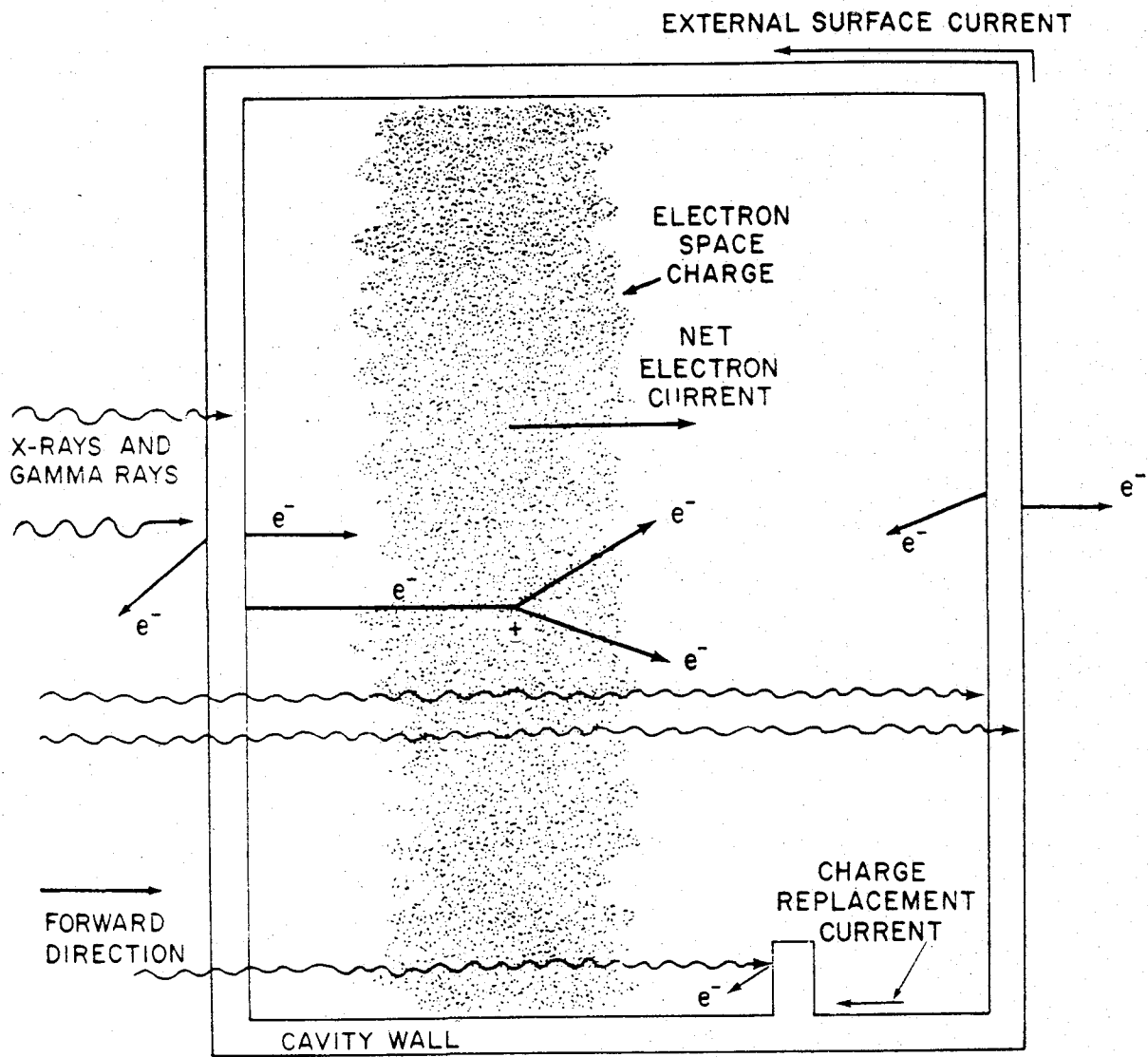


Figure 7-21 SGEMP Generation

[REDACTED]

It is possible that this evaluation procedure may be terminated after any given step. For example, consider an electronically very "hard" system for which the "threat" is specified as 4.2×10^4 joules/meter² (1 cal/cm²) received uniformly over a period of a year. By inspection, SGEMP is not a problem. At the other extreme, consider a system that is easily upset by small (milliamp), short duration (30 nsec) electrical pulses. If the threat for this system is 4.2×10^5 joules/meter² (10 cal/cm²) in a period of 100 nanoseconds, SGEMP may be a significant problem. An in-depth analytical/experimental program must be undertaken to make an evaluation of SGEMP effects.

Clearly, the above examples are extremes. They only serve to illustrate that an all encompassing definition of SGEMP problems is impossible because of the highly complex, system-specific nature of this phenomenon. Likewise, it is not possible to formulate a specific solution to the SGEMP threat for general application. Thus, the susceptibility and vulnerability of each system to SGEMP effects must be considered separately.

COMPUTER CODE DESCRIPTIONS

7-11 Code Utility

From the physical descriptions provided in the preceding paragraphs, it is apparent from the large number of variables involved that even approximate solutions to practical problems of interest demand a large investment in electronic computation. The complete problem of the coupling of the EMP from a specific detonation into the components of a specific system is an extremely complex problem. There are no computer codes which even remotely approach a treatment of the complex problem. As a consequence, various aspects of the EMP problem are

studied individually with the aid of existing codes, and good engineering judgment must be used to couple these various parts of the solution into a quantitative estimate of the effects of EMP upon a given system.

7-12 Code Classes

There are three general classes of computer codes in use: environment codes, system generated EMP codes, and circuit-analysis codes. The codes that are currently in use are described in the "DNA EMP (Electromagnetic Pulse) Handbook," Volume 4 (see bibliography).

SYSTEMS EFFECTS

7-13 System Definitions

Many systems that are physically different can be grouped together in terms of the EMP environments they will encounter. For this purpose it is useful to consider classification of systems in terms of operating altitude and nuclear hardness.

From the previous description of the EMP environment, the altitude categories suggested in Figure 7-22 are evident. It should be noted that certain systems may operate successively in more than one category.

For the purposes of this manual it is adequate to consider system hardness in only two categories. A hard system is one that has been designed to operate in some nuclear environment. A soft system is not so designed, and its hardness is due solely to its inherent design. For a ground system, the blast usually is considered to be the indicator of the nuclear hardness of the system. The dominant effect will change from blast to nuclear radiation, defined here in terms of the total dose in rad (Si), as the system altitude increases. A system is considered to be

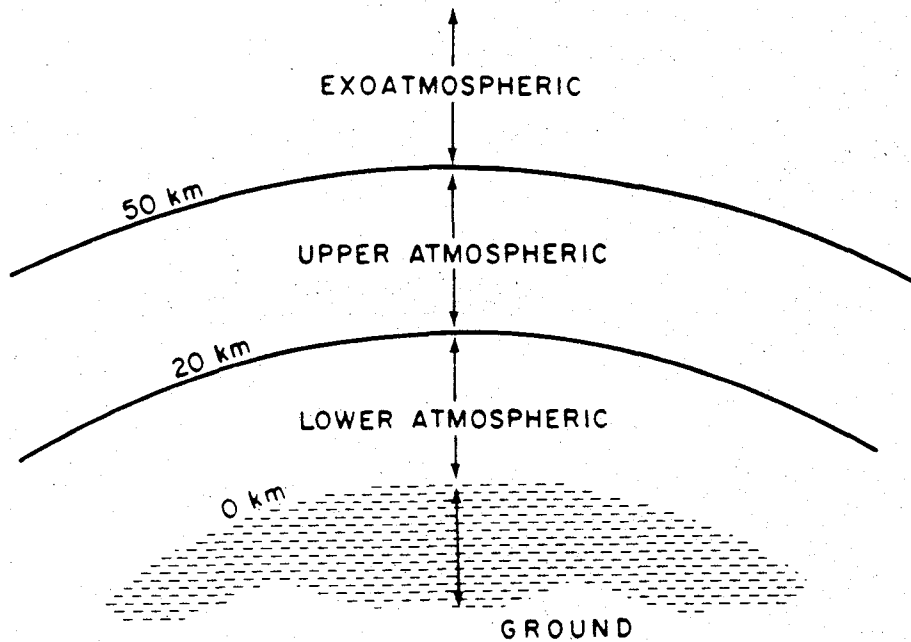
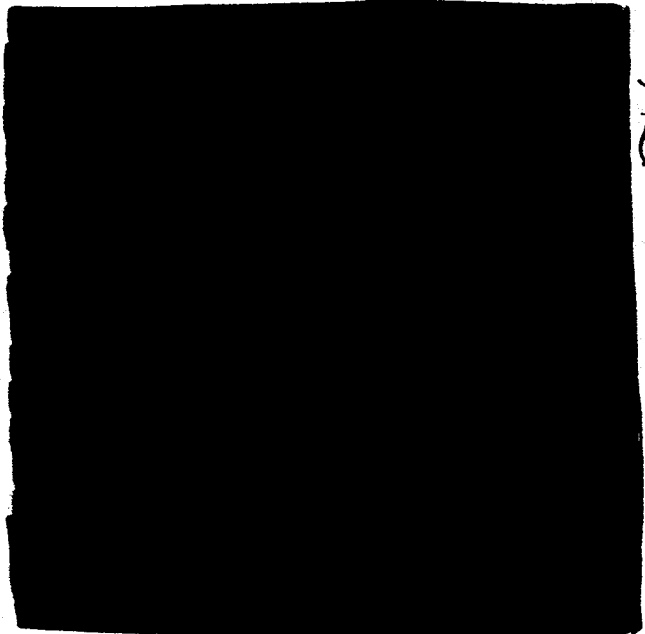


Figure 7-22 Categories of System Operation Regions

hard if it is built to withstand blast overpressures of about 70 kilopascals (10 psi) or more or a radiation dose of 1 rad (Si) or more. Corresponding figures for a soft system are 7 kilopascals (1 psi) or less and 0.1 rad (Si) or less. Systems marginal with respect to either criterion should be reviewed in both categories.

7-14 Threat Definition

DNA
(6)(1)



DNA
(6)(1)



		EMP ENVIRONMENT								
		DEPOSITION			RADIATION			PROPAGATION		
		SURFACE	AIR	HIGH ALTITUDE	SURFACE	AIR	HIGH ALTITUDE	SURFACE	AIR	HIGH ALTITUDE
MISSION	HARD	GROUND	X				X			
		LOWER ATMOSPHERIC		X			X			
		UPPER ATMOSPHERIC			X		X			
		EXO ATMOSPHERIC								X
	SOFT	GROUND			X		X			
		LOWER ATMOSPHERIC			X	X	X			
		UPPER ATMOSPHERIC					X			
		EXO ATMOSPHERIC								X

Figure 7-23 Mission/Environment Matrix



DNA
(6)(1)

Blocks are shaded in on the diagram on the basis of dominant environments for a given mission, not on the basis of whether EMP exists at all for that situation. Thus, based on the definitions given, Figure 7-23 may be used as a guide for which environments constitute a dominant threat for given situations of interest.

7-15 Effects Comparisons

It is well beyond the scope of this chapter to attempt meaningful effects comparisons for every system altitude, burst altitude, and environment combination for which EMP may be the dominant threat. However, it is instructive to consider one such combination in order to gain some impression of how the magnitude of the threat might be compared to other effects. Accordingly, the deposition region environment created by a surface burst will be examined with regard to the effects on hardened ground systems, a category in which the EMP threat may dominate according to Figure 7-23. As mentioned previously, the nuclear hardness of such a system is generally described in terms of its over-pressure level. Using this quantity as an indicator of hardness, the EMP field waveforms, peak values and frequency content for the principal field components B_ϕ , E_r , and E_θ , as defined in Figure 7-24 and the associated air conductivity waveforms and peak values will be examined.

The peak values as a function of over-pressure are considered first. Figures 7-25, 7-26, and 7-27 show these values for the three field components for two yields and two values of ground conductivity (σ_g). It should be kept in mind that a large shift in frequencies present can

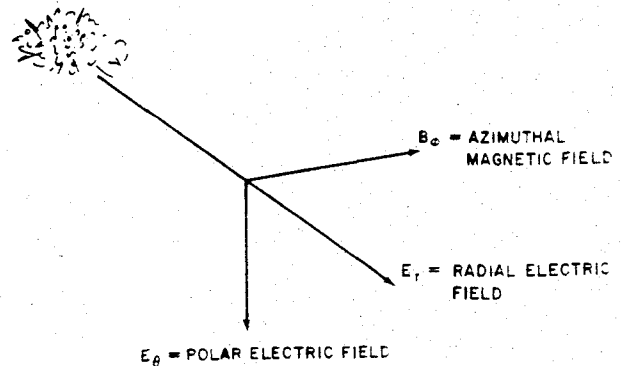


Figure 7-24 Field Directions of Ground-Burst EMP

occur between 70 and 7,000 kilopascals (10 and 100 psi). The coupling of systems to the fields in this intense region is complicated by the high air conductivity. Figure 7-28 shows how peak air conductivity varies with overpressure. It should be noted that the lower yield weapon produces higher conductivity for a given over-pressure level.

The variation of these same quantities in time for the 4,200 terajoules (1 MT) yield and a ground conductivity of 10^{-2} mho/m is illustrated next. The waveform for the B_ϕ component is shown for various overpressure levels in Figure 7-29, and the frequency spectrum is illustrated in Figure 7-30. Corresponding waveforms and spectra for E_r and E_θ components are shown in Figures 7-31, 7-32, 7-33, and 7-34. Finally, the corresponding air conductivity waveforms are presented in Figure 7-35.

It is apparent from these figures that meaningful effects comparisons can be made and presented to the systems designer for a given set of physical conditions. However, it is also clear that the results vary drastically with changes in

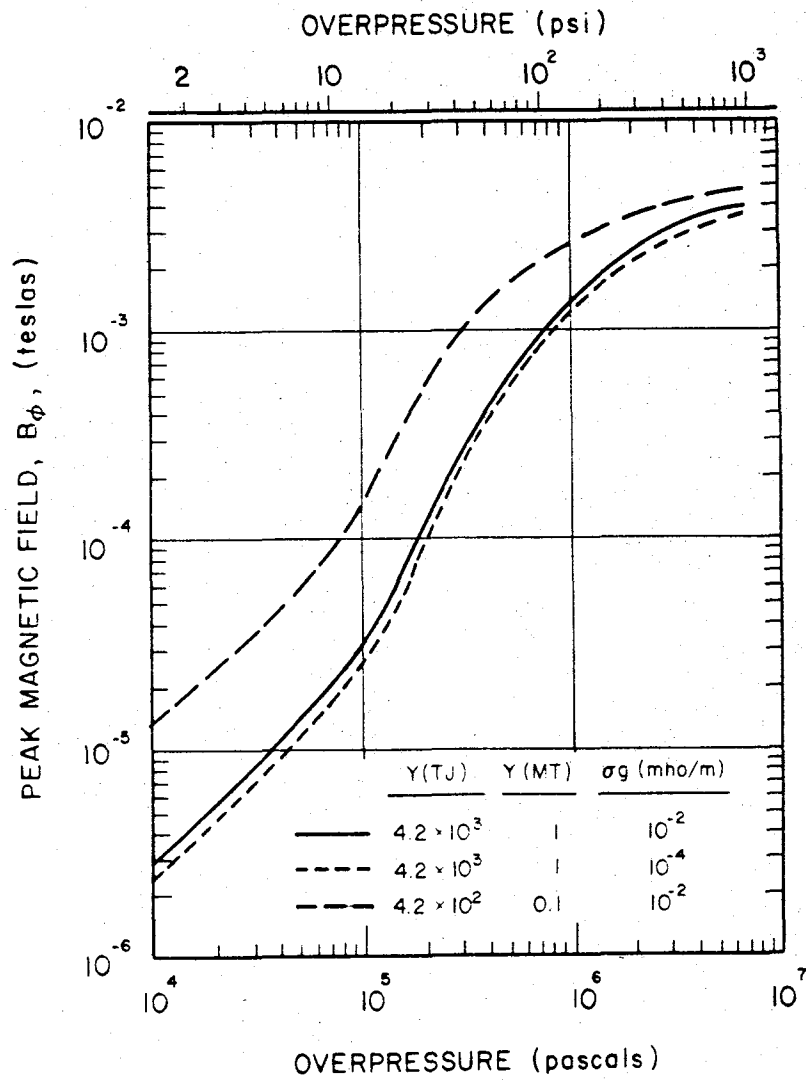


Figure 7-25 Peak Magnetic Field B_{ϕ} Versus Overpressure for Varying Ground Conductivities and Yields

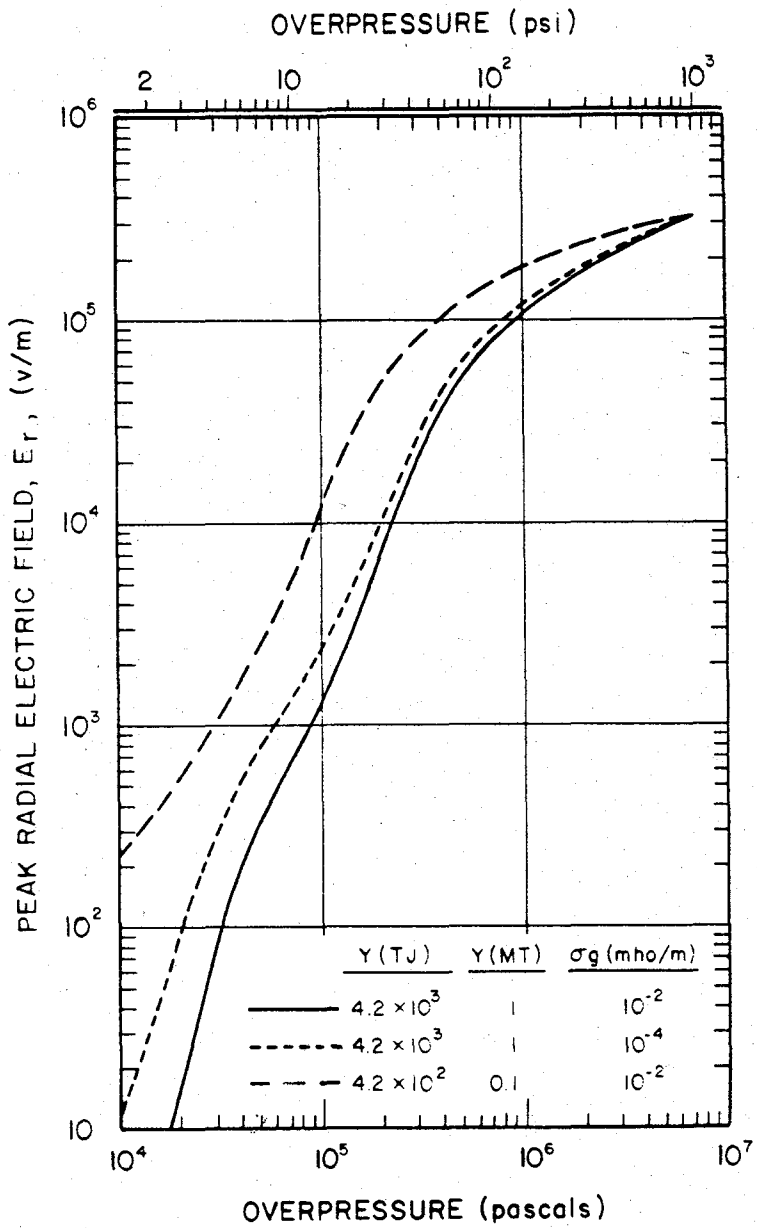


Figure 7-26 Peak Radial Electric Field E_r Versus Overpressure for Varying Ground Conductivities and Yields

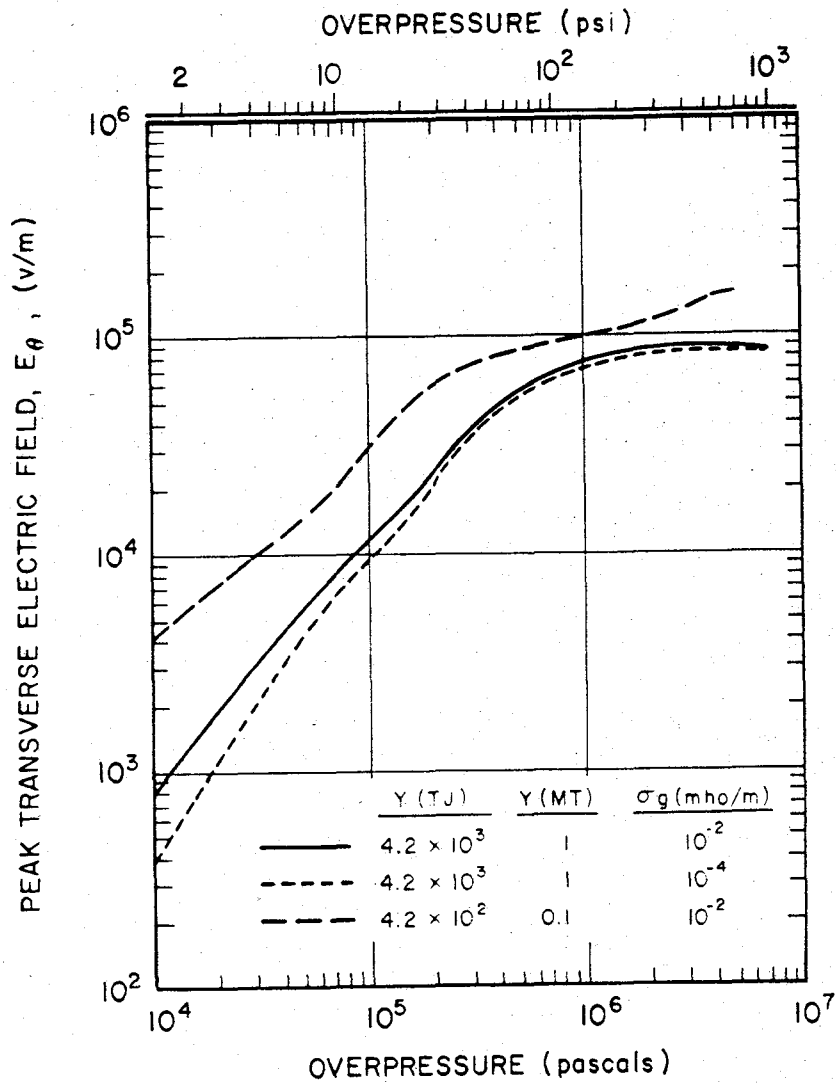


Figure 7-27 Peak Transverse Electric Field E_θ Versus Overpressure for Varying Ground Conductivities and Yields

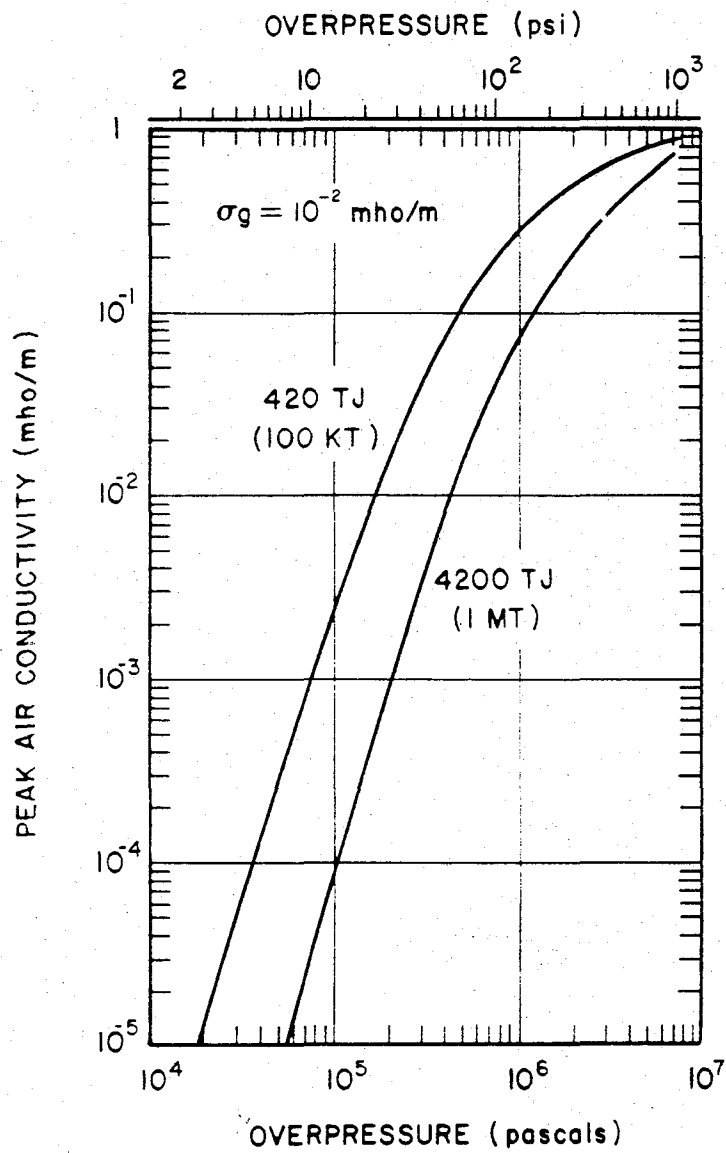


Figure 7-28 Peak Air Conductivity Versus Overpressure for Yields of 420 TJ (100 kt) and 4.2×10^3 TJ (1 Mt)

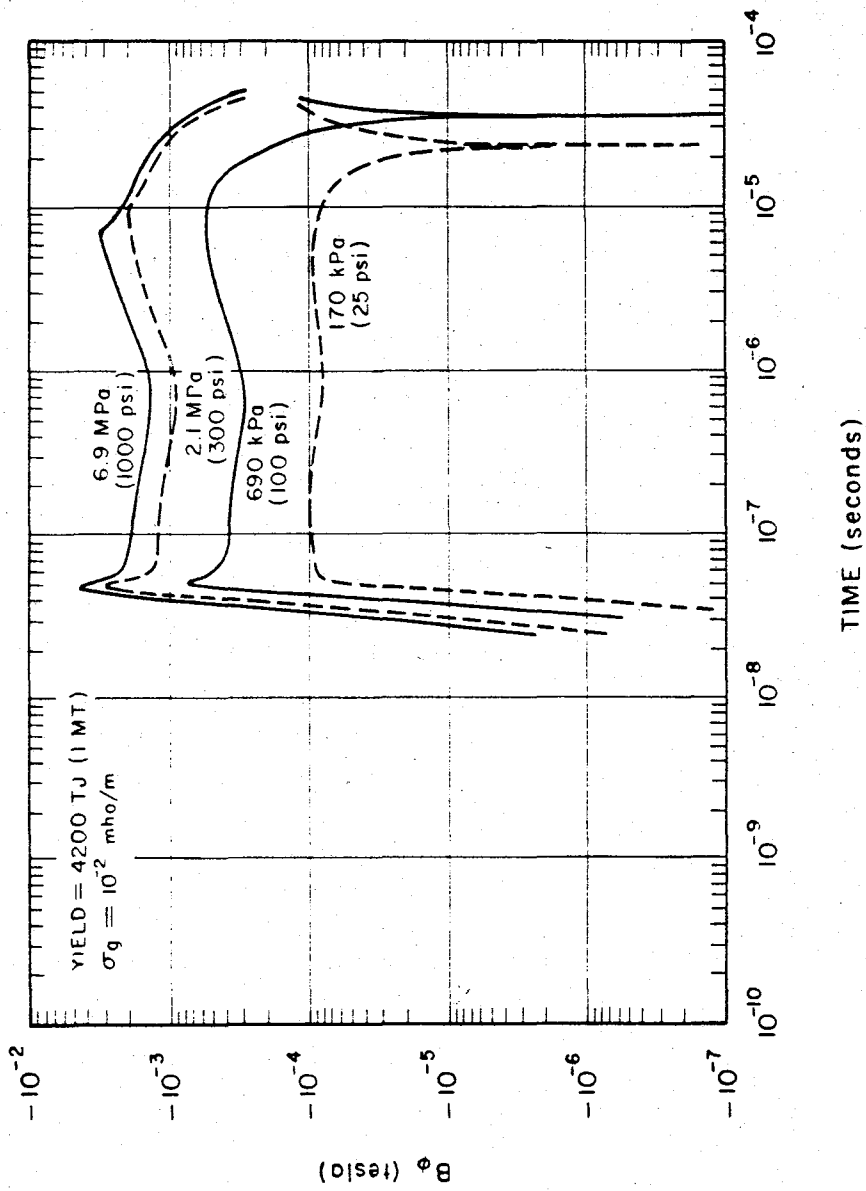


Figure 7-29 B_ϕ Time Waveform at the Air-Ground Interface for Several Pressure Levels

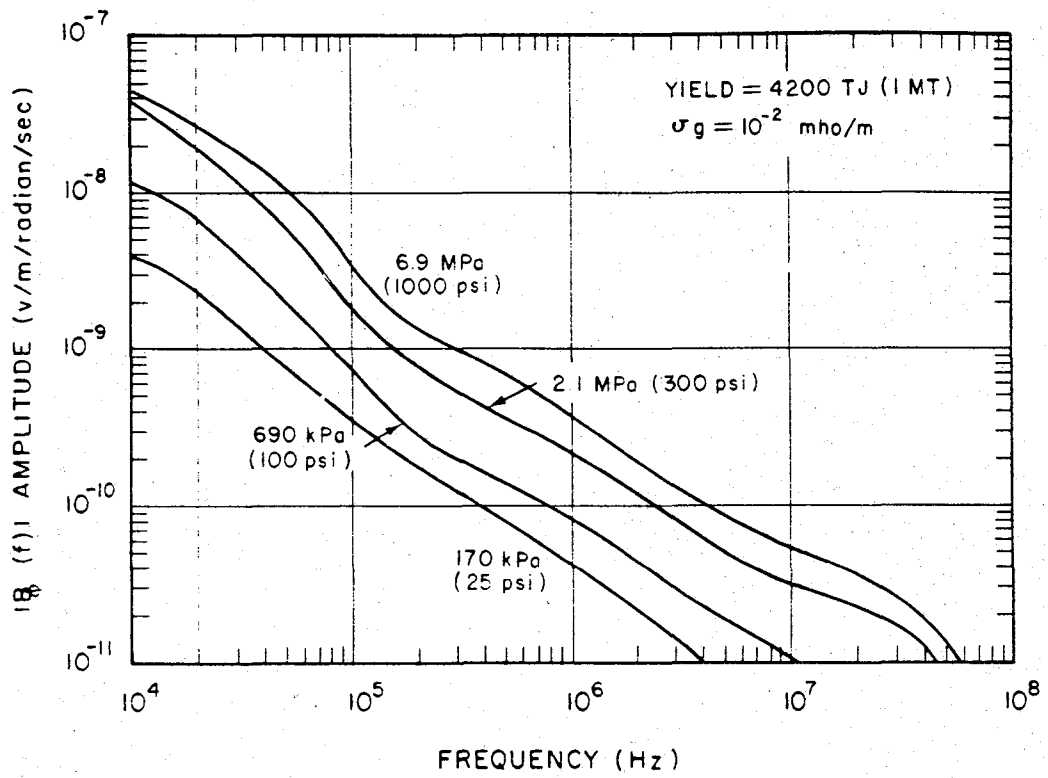


Figure 7-30 Fourier Amplitude of B_z Waveform of Figure 7-29

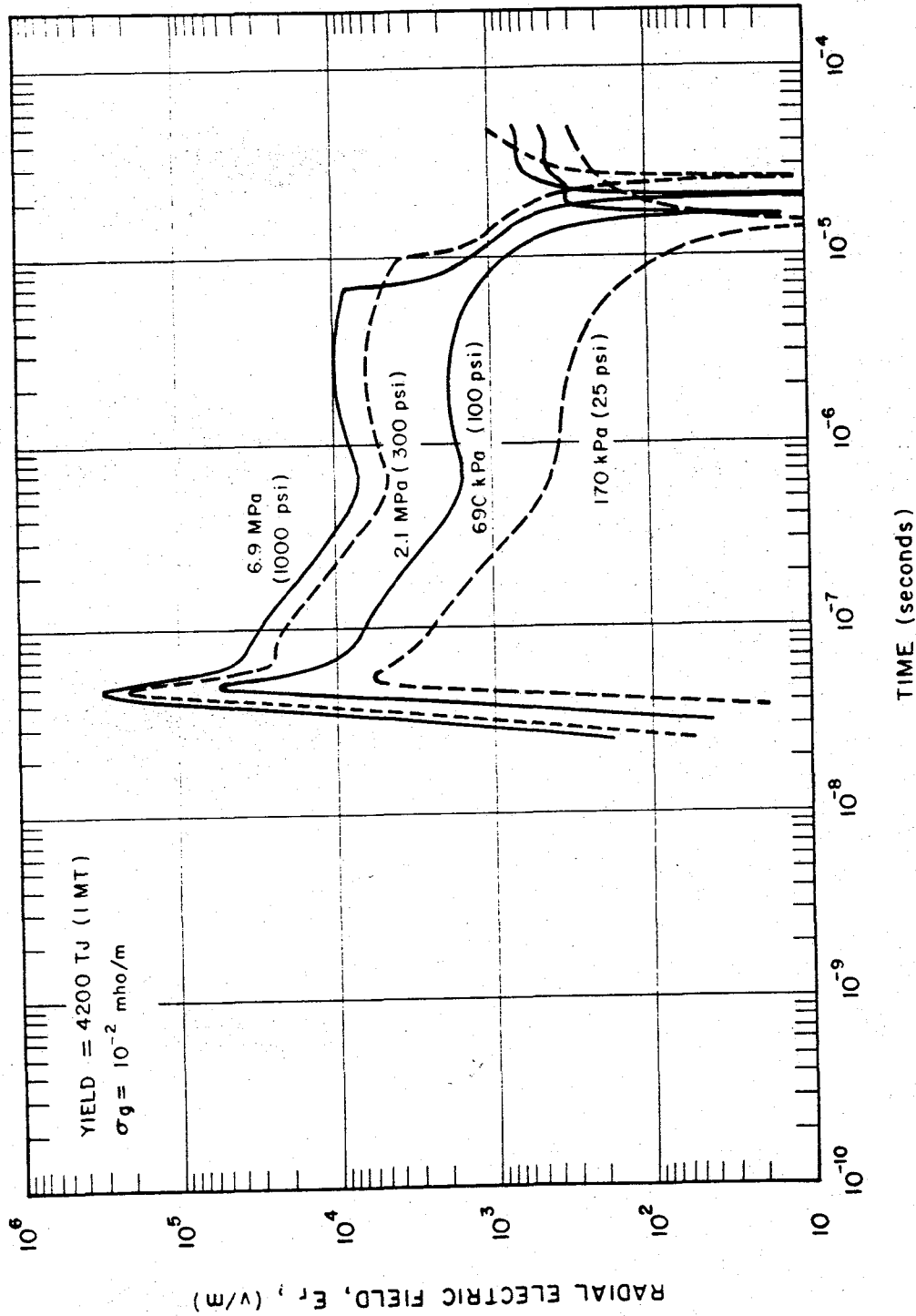


Figure 7-31 E_r Time Waveform at the Air-Ground Interface for Several Pressure Levels, $\sigma_g = 10^{-2}$ mho/m

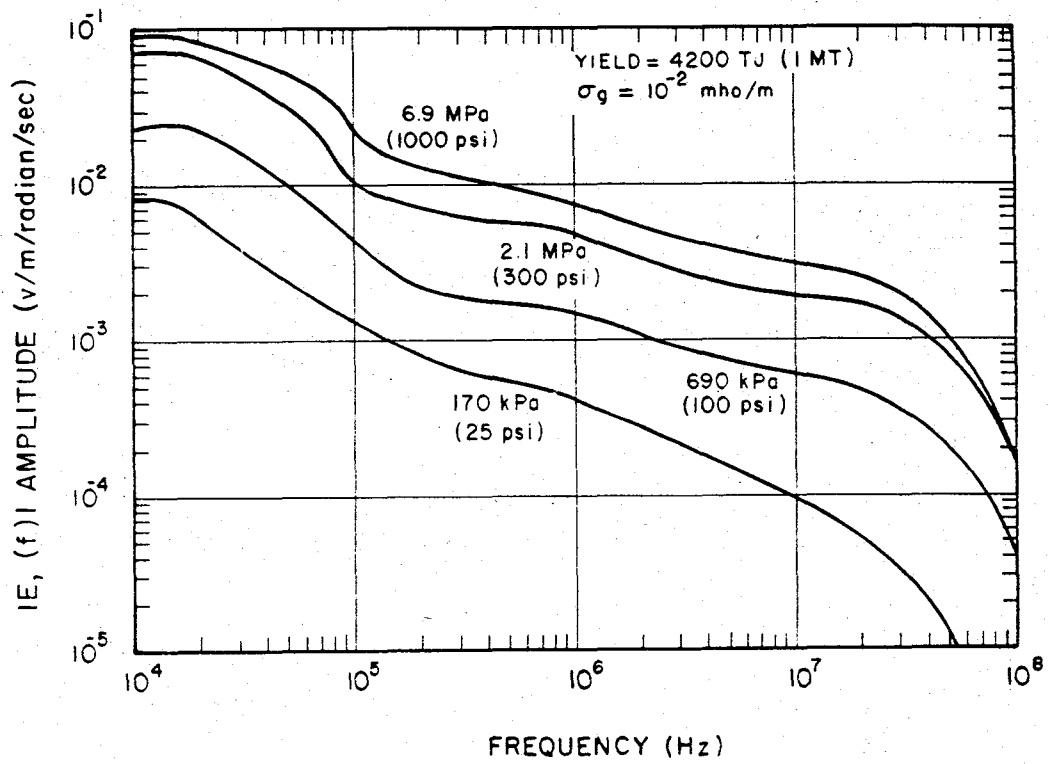


Figure 7-32 Fourier Amplitude of E_r Waveform of Figure 7-31

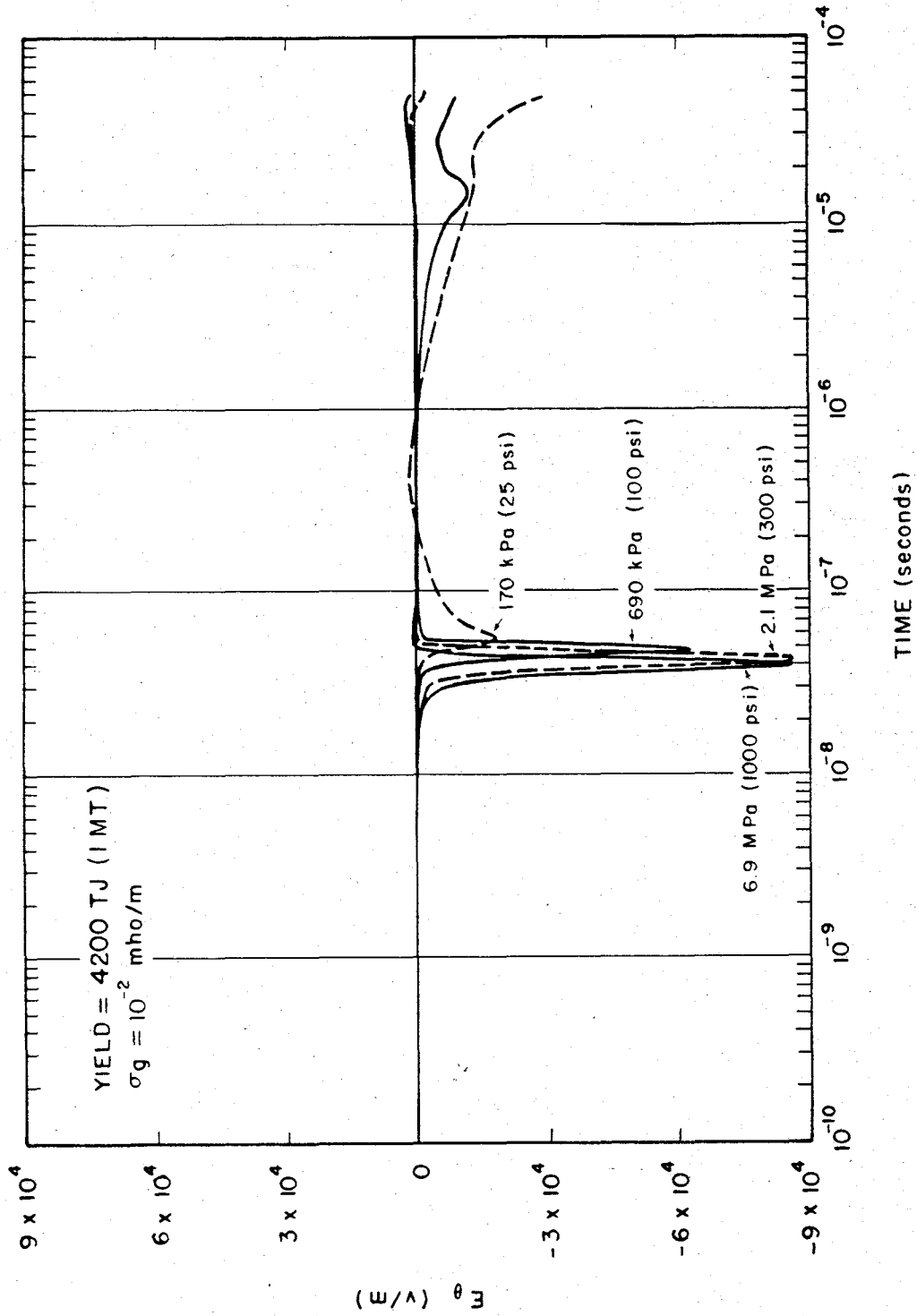


Figure 7-33 E_θ Time Waveform at the Air-Ground Interface for Several Pressure Levels, $\sigma_g = 10^{-2}$ mho/m

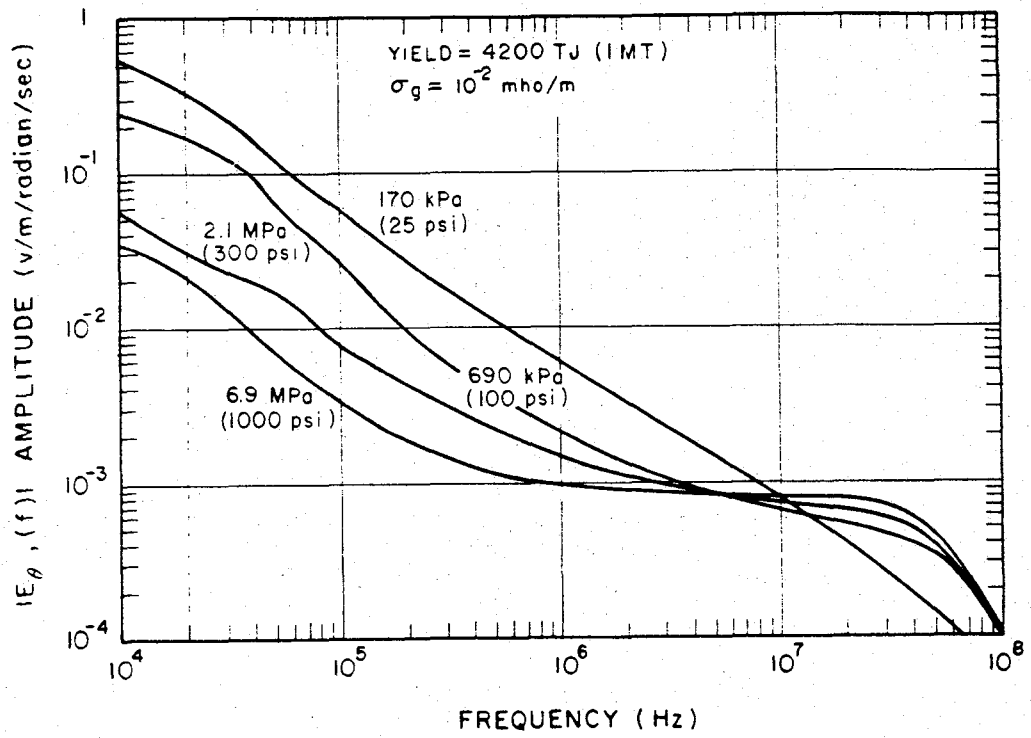
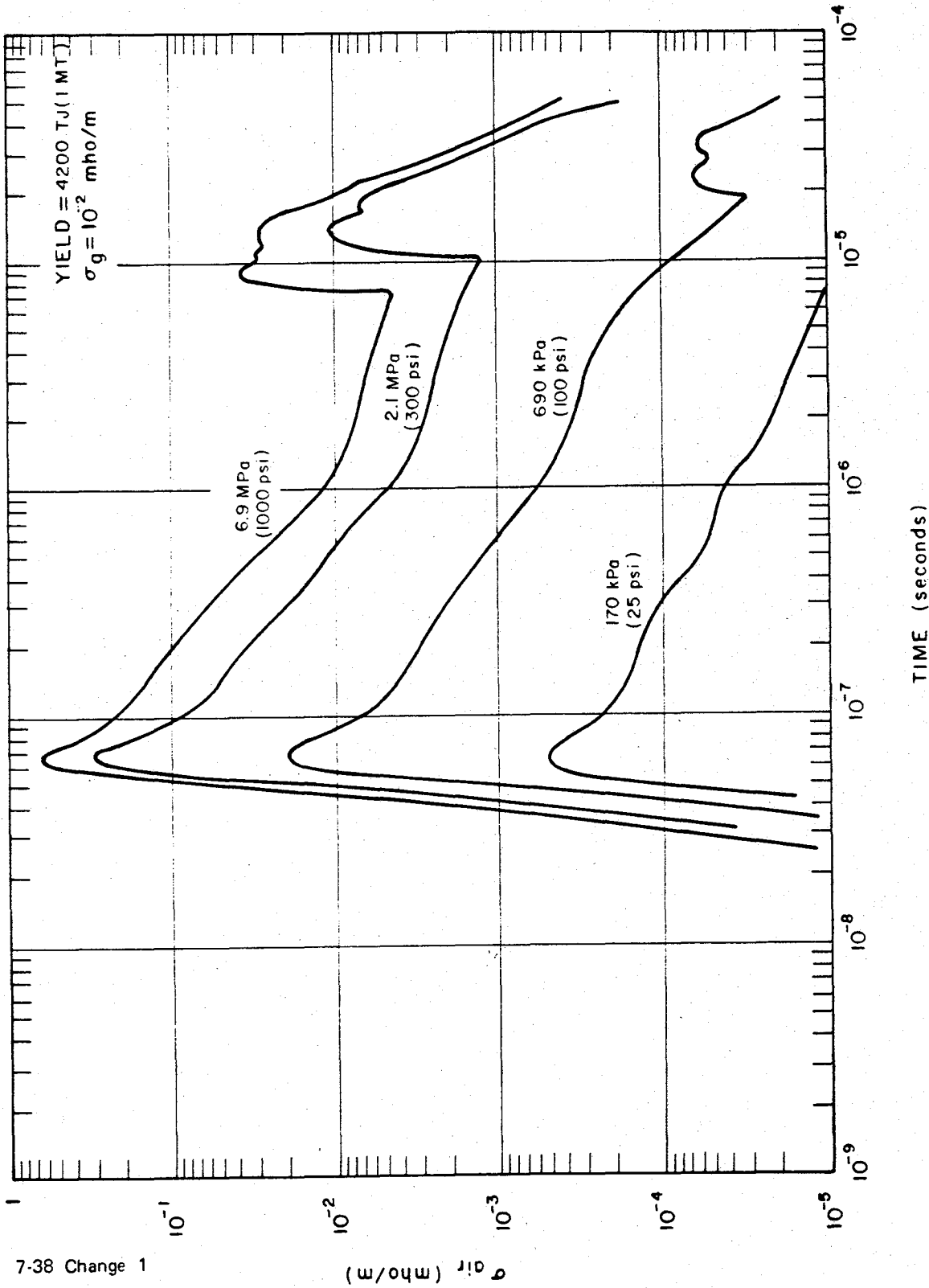




Figure 7-34 Fourier Amplitude of E_θ Waveform of Figure 7-33



7-38 Change 1

Figure 7-35 Air Conductivity Time Waveforms at the Air-Ground Interface for Several Pressure Levels, $\sigma_g = 10^{-2}$ mho/m



the conditions, and that the very many combinations possible in the conditions preclude concise generalizations to cover every situation. Strictly speaking, a system imbedded in the deposition region must be included as part of the environment itself in formulating the problem. This limitation should be kept in mind while examining the figures described.

[REDACTED]

BIBLIOGRAPHY

DNA EMP (Electromagnetic Pulse) Handbook [REDACTED] DNA 2114H-1, DNA 2114H-2, DNA 2114H-3, DNA 2114H-4. Defense Nuclear Agency, Washington, D.C., August 1976. (I, II, IV - [REDACTED] III - [REDACTED])

EMP Simulator Study [REDACTED] DASA 2049, DASIAC SR-92, DASIAC, Santa Barbara, California, May 1968 [REDACTED]

Glasstone, S. and P. J. Dolan, eds., *The Effects of Nuclear Weapons*, Third Edition, U.S. Department of Defense and U.S. Department of Energy, December 1977 [REDACTED]

Jordan, T. M., et al., *Prediction of Internal Electromagnetic Pulse* [REDACTED] DNA 2966D, Defense Nuclear Agency, Washington, D.C., August 1972 [REDACTED]

Longmire, C. L., *Ground Fields and Cable Currents Produced by Electromagnetic Pulse from a Surface Nuclear Burst* [REDACTED] DASA 1913, DASIAC SR-54, DASIAC, Santa Barbara, California, March 1968 [REDACTED]

Proceedings: DASA EMP Technical Conference - 1969 [REDACTED] DASA 2280, DASIAC SR-91, DASIAC, Santa Barbara, California, March 1969 [REDACTED]

Schlegel, G. K., M. A. Messier and W. A. Radasky, (edited by W. C. Hart), *Electromagnetic Pulse Environment Handbook* [REDACTED] AFWL EMP PHENOMENOLOGY 1-1, Air Force Weapons Laboratory, Albuquerque, N.M., January 1972 [REDACTED]

Tompkins, J. E., and J. A. Rosado, *Internal Electromagnetic Pulse: Electric and Magnetic Fields in Complex Enclosures* [REDACTED] HDL-TR-1500, Harry Diamond Laboratories, Washington, D.C., June 1970 [REDACTED]